Rheological Behavior of Polymer–Clay Nanocomposite Hydrogels: Effect of Nanoscale Interactions

Suzan Abdurrahmanoglu,[1] Oguz Okay[2]

[1]*Department of Chemistry, Marmara University, Kadikoy, Istanbul 34722, Turkey*
[2]*Department of Chemistry, Istanbul Technical University, Maslak, Istanbul 34469, Turkey*

Received 24 May 2009; accepted 31 October 2009
DOI 10.1002/app.31705
Published online 14 January 2010 in Wiley InterScience (www.interscience.wiley.com).

ABSTRACT: This research highlights different viscoelastic responses of polymer–clay nanocomposite hydrogels depending on the type of the monomer used in their preparation. Polymerization reactions of *N*,*N*-dimethylacrylamide (DMA), *N*-isopropylacrylamide (NIPA), and acrylamide (AAm) in aqueous clay (Laponite) dispersions have been investigated by rheometry using oscillatory deformation tests. The gelation profile of AAm polymerization obeys typical gelation kinetics, while a reverse behavior was observed during the DMA or NIPA polymerizations. In the latter cases, after an abrupt increase in elastic and viscous moduli at the start of the reaction, they both decrease continuously during the whole course of the gelation process. Creep-recovery tests performed on the final hydrogels indicate that the time-dependent viscoelastic response of the gels derived from AAm is distinctly different from the other gels. The retardation time of AAm gel is about twice that of DMA or NIPA gels indicating higher mobility of the crosslink zones in the former gel. As a consequence, a larger amount of energy is dissipated during the deformation of nanocomposite hydrogels based on AAm. Different extent of interactions between the clay particles and the monomers explains the results of observations. © 2010 Wiley Periodicals, Inc. J Appl Polym Sci 116: 2328–2335, 2010

Key words: nanocomposite hydrogels; clay; rheology

INTRODUCTION

In contrast to many biological gel composites, most synthetic hydrogels are fragile materials when handled in the swollen state.[1,2] Design of hydrogels with a good mechanical performance is thus critically important in their technological applications. Haraguchi et al. prepared such hydrogels through the *in situ* polymerization of *N*,*N*-dimethylacrylamide (DMA) or *N*-isopropylacrylamide (NIPA) in aqueous solutions of Laponite as a physical crosslinker, replacing the traditional chemical crosslinkers.[3–6] Laponite, a synthetic hectorite clay, when suspended in water forms disk-like particles with a thickness of 1 nm, a diameter of about 25 nm, and a negative surface charge density stabilizing dispersions in water.[7–9] It was shown that the nanocomposite hydrogels formed using Laponite as a crosslinker exhibit extraordinary mechanical toughness, tensile moduli, and tensile strengths.[3–6] This unusual feature was explained with the uniform distribution of Laponite particles within the hydrogel matrix as well as with the action of the nanoparticles as a multifunctional crosslinker due to strong interactions at the clay–polymer interface on a nanoscale level.

Nanocomposite hydrogels mentioned above were exclusively prepared from the monomers DMA or NIPA, i.e., from two hydrophobically modified acrylamides. Our preliminary experiments showed that, although the hydrogels based on DMA or NIPA exhibit superior mechanical properties, those prepared using acrylamide (AAm) do not show such properties. For example, nanocomposite DMA and NIPA hydrogels prepared at a monomer concentration of 5 w/v % and in the presence of 6% Laponite exhibited excellent tensile mechanical properties, as reported by Haraguchi et al.[6] However, when acrylamide (AAm) is used as the monomer, the nanocomposite gels formed suffer from mechanically instability and they flowed under gravity. Indeed, our previous uniaxial compression measurements also showed that the hydrogels based on DMA or NIPA exhibit much larger moduli of elasticity compared to the hydrogels based on AAm monomer.[10] This suggests that the hydrophobic modification of AAm is a requirement for obtaining Laponite hydrogels of high toughness. We have to note that, at a higher monomer concentration ($\geq$10 w/v %), nanocomposite hydrogels with a high extensibility were also obtained recently using AAm monomer.[11]

The focus of this research is on understanding the roles of nanoscale structures and interactions in

Correspondence to: O. Okay (okayo@itu.edu.tr).
Contract grant sponsor: Scientific and Technical Research Council of Turkey (TUBITAK); contract grant number: TBAG 105T246.

determining the macroscopic properties of nanocomposite hydrogels. In this work, we monitored the gelation reactions of AAm, DMA, and NIPA in aqueous Laponite dispersions by rheometry using oscillatory deformation tests. The complex shear modulus G^* measured can be resolved into its real and imaginary components, i.e., $G^* = G' + iG''$, where the elastic modulus G' is a measure of the reversibly stored deformation energy, and the viscous modulus G'' represents a measure of the irreversibly dissipated energy during one cycle. As the nature of physical crosslinks also affects the time-dependent changes in strain in response to stress, the hydrogels were also studied with time-domain rheological experiments. In particular, creep compliance for nanocomposite hydrogels was evaluated by applying an "instantaneous" stress and measuring the time-dependent increase of strain. As will be seen later, nanoscale interactions between Laponite and hydrophobically modified AAm are much stronger than those between Laponite and AAm, which are responsible for the improved mechanical properties of nanocomposite DMA or NIPA hydrogels.

EXPERIMENTAL

Materials

Acrylamide (AAm, Merck), *N*,*N*-dimethylacrylamide (DMA, Aldrich), *N*-isopropylacrylamide (NIPA, Aldrich), ammonium persulfate (APS, Merck), and *N*,*N*,*N*′,*N*′-tetramethylethylenediamine (TEMED, Merck) were used as received. The synthetic hectorite clay, Laponite XLS $[Na^+_{0.7}(Si_8Mg_{5.5}Li_{0.3})O_{20}(OH)_4]^{0.7-}$, modified with pyrophosphate ions ($P_2O_7^{4-}$)) was provided by Rockwood. Suspensions of Laponite XLS were prepared by dispersing the white powder at the preset concentrations in deionized water with vigorous stirring for one week.

Polymerization

Nanocomposite hydrogels were prepared in a similar manner to that reported previously,[9,10,12] i.e., by free-radical polymerization of the monomers in aqueous clay suspensions using APS - TEMED redox initiator system at 25°C. The initial concentration of the monomer AAm, DMA, and NIPA was set to 5 w/v % (g monomer / 100 mL solution), while the Laponite concentration was varied between 1 and 7%. The monomer AAm, DMA, or NIPA and the accelerator TEMED (0.25 v/v %) were first dissolved in Laponite XLS aqueous suspensions. After bubbling nitrogen, the initiator APS (3.51 m*M*) was added to the reaction solution and the polymerization was conducted between the parallel plates of the rheometer at 25°C.

In the following paragraphs, nanocomposite hydrogels prepared from AAm, DMA, and NIPA monomers in aqueous Laponite dispersions were designated as AAm, DMA, and NIPA gels, respectively, while the indicated amounts of Laponite (Laponite %) correspond to the mass of Laponite in 100 mL reaction solution.

Rheological measurements

Gelation reactions and the rheological properties of the resulting gels were monitored within the rheometer (Gemini 150 Rheometer system, Bohlin Instruments) equipped with a Peltier device for temperature control. The upper plate (diameter 40 mm) was set at a distance of 500 μm before the onset of the reactions, i.e., during the induction period. During all rheological measurements, a solvent trap was used to minimize the evaporation. A frequency of $\omega = 1$ Hz and a deformation amplitude $\gamma^o = 0.01$ were selected to ensure that the oscillatory deformation is within the linear regime. The reactions were monitored in the rheometer at 25°C up to a reaction time of about 2 h to avoid the effect of the solvent evaporation. Thereafter, frequency-sweep tests at $\gamma^o = 0.01$ were carried out over the frequency range 0.01–30 Hz.

Creep and creep-recovery experiments were performed using gel samples prepared within the rheometer after a reaction time of 3 h. Creep compliances $J_c(t)$ were evaluated by applying a constant shear stress τ_0 and measuring the time-dependent increase of the strain γ for 4000 s. After 4000 s, the shear stress was set to zero and the recovery compliances $J_r(t)$ were measured also during 4000 s.

RESULTS AND DISCUSSION

As mentioned in the Introduction, at a monomer concentration of 5 w/v %, hydrophobic modification of AAm monomer is a requirement for obtaining nanocomposite hydrogels of high toughness. To highlight the effects responsible for this behavior, rheological measurements were conducted both during the formation process of the nanocomposite hydrogels as well as after their preparation states. Formation of nanocomposite hydrogels through the polymerization of AAm, DMA, and NIPA in aqueous Laponite dispersions was first monitored by rheometry at a fixed frequency (1 Hz) and strain amplitude γ^o (0.01). In Figure 1, the elastic modulus G' (filled symbols), the viscous modulus G'' (open symbols), and the loss factor *tan* δ (dotted curve), which is the ratio of G'' to G', are shown as a function of the reaction time during AAm (A) and DMA polymerizations (B). Laponite contents are 6% Laponite in both cases. Double-logarithmic plots were chosen

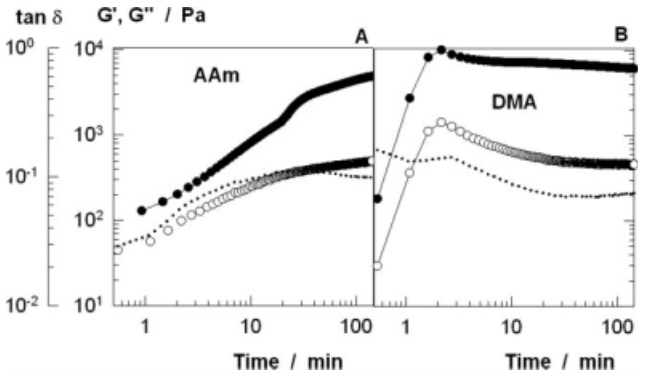

Figure 1 Elastic modulus G' (●), viscous modulus G'' (○), and *tan* δ (dotted curve) during the AAm (A) and DMA polymerizations (B) in 6% Laponite dispersion shown as a function of the reaction time.

for clearer representation of the changes in the dynamic moduli of the reaction systems at short reaction times. In the absence of Laponite (not shown), both moduli of the reaction solution remain below 10^1 Pa and the system exhibits liquid-like response during the whole course of the polymerization. In the presence of Laponite, however, viscoelastic gels with a modulus of elasticity in the order of kPa's were obtained, indicating formation of elastically effective junction zones between the polymer segments and the nanoparticles.

Figure 1 clearly shows that the gelation profiles of DMA and AAm in aqueous Laponite dispersions are completely different. During the AAm polymerization, both moduli and *tan* δ gradually increase and then, they approach plateau values at longer times. Thus, AAm polymerization in Laponite dispersion obeys typical gelation kinetics, as also observed during the free-radical crosslinking copolymerization of AAm with chemical crosslinkers.[13] However, a reverse behavior was observed during the DMA polymerization [Fig. 1(B)]; after an abrupt increase in both G' and G'' at the start of the reaction, they both decrease continuously during the whole course of the gelation process. For example, $G' = 10$ kPa and $G'' = 1.4$ kPa after 2 min, while they become 6.1 and 0.5 kPa, respectively, after 2.5 h. To our knowledge, such a gelation profile has not been observed before during the crosslinking reactions. Figure 1(B) also shows that the decrease of both moduli is accompanied by a continuous decrease in the loss factor *tan* δ and it approaches a limiting value of 0.07 at longer times. As the quantity *tan* δ represents the ratio of dissipated energy to stored energy during one deformation cycle, the results suggest that, although the elastic modulus decreases with time, the reaction system behaves increasingly solid-like as the time is increased. This indicates the decrease in the number of elastically ineffective polymer chains, i.e., those chains with free ends or chains with both ends attached to the same particle surface. Although to a lesser extent, the gelation profile of NIPA (not shown in Fig. 1) was similar to that of DMA.

Similar results such as those given in Figure 1 were also observed over the whole range of Laponite concentrations investigated, namely between 1 and 7%. Figure 2 shows G' and G'' vs reaction time plots for DMA, NIPA, and AAm polymerizations in aqueous dispersions of 1 to 5% Laponite. While during the AAm polymerization the moduli gradually increase during gelation, DMA and NIPA polymerizations are

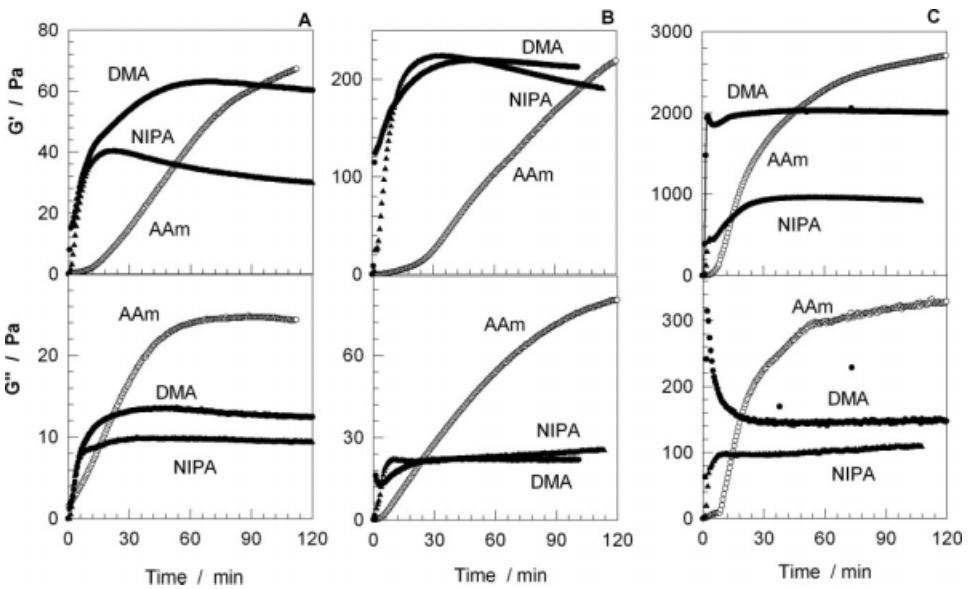

Figure 2 Elastic modulus G', and viscous modulus G'' during the polymerizations of AAm (open symbols), DMA (filled circles), and NIPA (filled triangles) in Laponite dispersions shown as a function of the reaction time. Laponite % = 1 (A), 2 (B), and 5 (C).

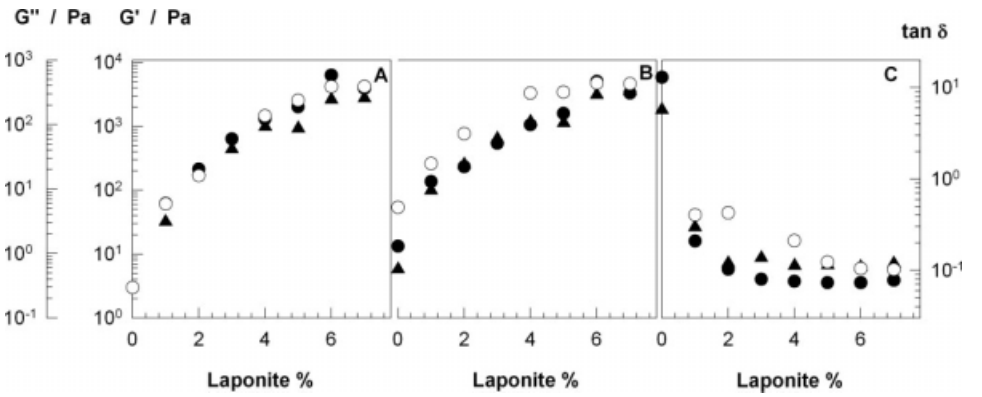

Figure 3 Elastic modulus G' (A), the viscous modulus G'' (B), and *tan* δ (C) of nanocomposite hydrogels after a reaction time of 90 min shown as a function of their Laponite contents. DMA (●), NIPA (▲), and AAm gels (○).

characterized by the rapid increase of G' and G'', followed by their decrease at longer times. Note that the initial rise of the moduli is less dramatic for Laponite contents below its critical overlap concentration c*, which is 4.5 ± 1% in water.[12,14] In Figure 3, the values of G', G'' and *tan* δ recorded after a reaction time of 90 min are plotted against the Laponite concentration. Although both moduli and *tan* δ of nanocomposite hydrogels are in the same order of magnitude, AAm gels exhibit slightly larger viscous moduli and thus, larger loss factor, indicating that these gels are more viscous as compared to DMA or NIPA gels. Further, among the nanocomposite hydrogels, those prepared using NIPA exhibit the lowest elastic moduli G', i.e., the lowest effective crosslink densities.

After a reaction time of 2 h, frequency-sweep tests at $\gamma^o = 0.01$ were carried out over the frequency range 0.01–30 Hz. Figure 4 shows the frequency dependence of G' (filled symbols) and G'' (open symbols) for the nanocomposite hydrogels with 4 and 6% Laponite. For all the Laponite hydrogels, G' is larger than G'' and shows a plateaulike behavior, with a height increasing with the Laponite concentration, indicating formation of viscoelastic gels. Comparison of the mechanical spectra shows that they exhibit similar behavior except that, in the high frequency range, G'' of AAm hydrogels increases with increasing frequency. High frequency rise in G'' reflects fast relaxation processes and is typical viscous behavior of gels formed by temporary (breakable) junction zones.[15] Such relaxation processes

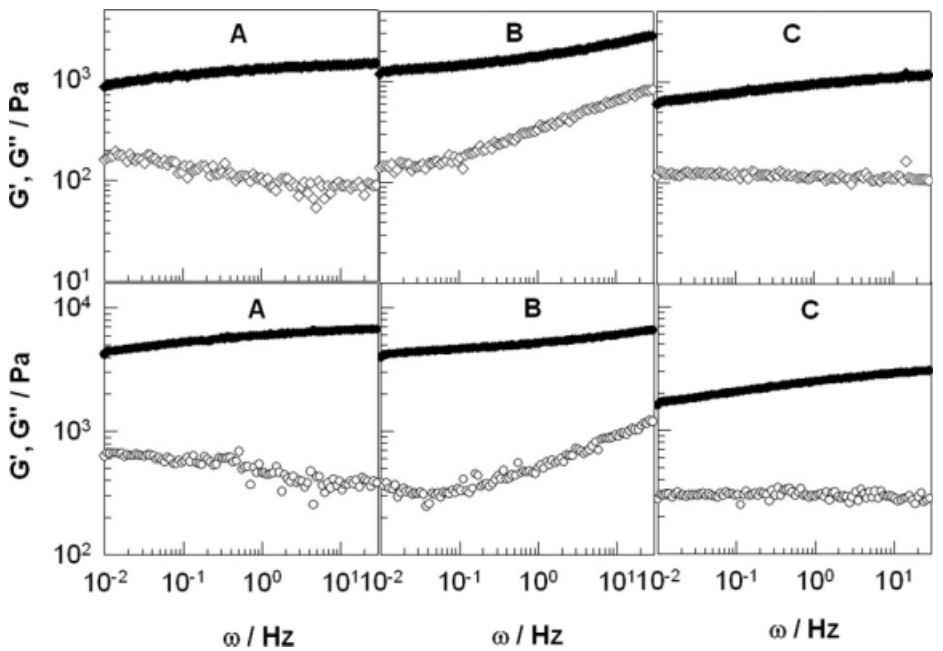

Figure 4 Elastic moduli G' (filled symbols) and viscous moduli G'' (open symbols) shown as a function of the frequency ω measured after 2 h of reaction time. Laponite = 4% (upper graphs) and 6% (lower graphs). DMA (A), AAm (B), and NIPA gels (C).

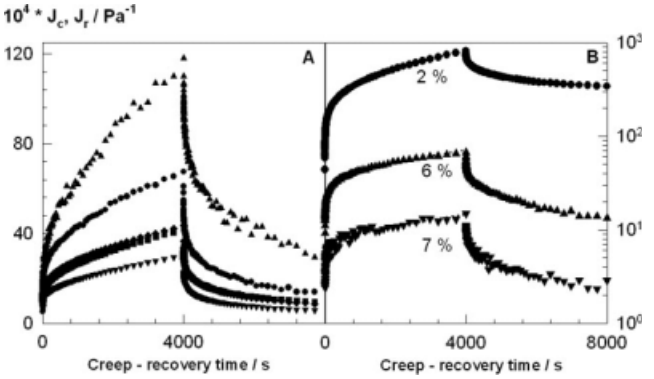

Figure 5 Creep-recovery curves of nanocomposite NIPA hydrogels. Creep $J_c(t)$ and recovery compliances $J_r(t)$ are shown as a function of creep (0–4000 s) and recovery times (4000–8000 s). (A): NIPA gels with 6% Laponite under a constant stress τ_0 of 1 (▲), 5 (●), 20 (■), 30 (◆), and 50 Pa(▼). (B): NIPA gels with various contents of Laponite indicated. $\tau_0 = 5$ Pa.

have been observed in transient networks due to the localized motion of hydrophobic species in associations.[15–19] In the present case, the extensive rearrangement of the highly entangled polyacrylamide chains close to the Laponite surface in the experimental time scale may contribute this behavior.

The time-dependent viscoelastic properties of nanocomposite hydrogels and their internal structure were investigated by creep-recovery experiments. The creep compliance was analyzed by means of the Burger model composed of a Maxwell element in series with one Kelvin–Voigt element, i.e.,

$$J_c(t) = J_o + J_1[1 - \exp(-t/\tau)] + \frac{t}{\eta} \qquad (1)$$

where $J_c(t)$ is the measured compliance at time t, J_0, and J_1 are the compliances of the Maxwell and Kelvin–Voigt springs corresponding to the instantaneous and retarded compliances, respectively, τ is the retardation time, and η is the Newtonian viscosity.[20]

Figure 5(A,B) show typical creep-recovery curves of nanocomposite NIPA gels after a preparation time of 3 h. Here, the values of creep compliance $J_c(t)$ are shown as a function of creep time t between 0 and 4000 s. For the interval $4000 < t < 8000$ s, recovery compliance $J_r(t)$ is represented. Each creep curve is characterized by an initial elastic response corresponding to the instantaneous creep compliance J_0, followed by a time-dependent creep region related to a viscoelastic response. It must be noted that the creep time selected was not sufficient to reach the terminal flow zone, which is characterized by a double-logarithmic slope of one. Higher creep times were not applied to prevent solvent evaporation. Further, sudden removal of the applied stress τ_0 at time $t = 4000$ s allows a reversible deformation that partially recovers the initial shape of the gel. The recoverable deformation, γ %, was characterized by the recoverable compliance, determined by subtracting the residual compliance at the end of the recovery period from the maximum compliance reached at the end of the creep period. Figure 5(A) shows the behavior of NIPA gels with 6% Laponite measured under various applied stresses τ_0 between 1 and 50 Pa. Each test was conducted on freshly prepared NIPA gels within the rheometer. With increasing τ_0, the instantaneous compliance J_0 and the slope of the creep curves at longer times decrease, indicating increasing pure elastic response of the gels and their increased viscosities. Removal of the applied stress at time $t = 4000$ s recovers 75– 81% of the strain for $\tau_0 = 1$ and 50 Pa, respectively. Figure 5(B) shows the behavior of NIPA gels at various levels of Laponite under $\tau_0 = 5$ Pa. Semi-logarithmic plot was chosen for clearer representation of the changes in the compliances at high Laponite contents. With increasing Laponite concentration, the instantaneous compliance decreases, that is, the elastic modulus increases, which is in accord with the previous results [Figs 3(A) and 4]. Further, as the Laponite content is increased from 2 to 7%, recoverable deformation γ % also increases from 58 to about 80% indicating increasing elastic response of the nanocomposite hydrogels.

Results in Figure 5(A) reveals that the time-dependent viscoelastic behavior of gels depends on the applied stress τ_0, i.e., on the maximum strain γ_{max} reached at the end of the creep period; γ_{max} increased from 0.012 to 0.15 with increasing τ_0 from 1 to 50 Pa. To compare the characteristics of the nanocomposite hydrogels with each other, creep-recovery measurements were performed under the condition of a fixed maximum strain γ_{max} by suitably adjusting the applied stress τ_0. Figure 6 compares creep-recovery curves of NIPA, DMA, and AAm gels with 6% Laponite and for $\gamma_{max} = 0.093 \pm 0.008$, which is within the linear viscoelastic region for all of the samples analyzed. The fitting of the creep data to eq. (1) provided satisfactory agreement and is also shown in the figure by the dotted curves; the values of the parameters with the errors of the fit are collected in Table I. It is seen that the instantaneous compliance component J_0 of NIPA gel is much larger, i.e., its elastic modulus is much smaller than the other gels, which is in agreement with the observed tendency of G' noted earlier (see also lower graphs in Fig. 4). As the viscosity η at a given polymer concentration increases with the crosslink density, η of NIPA gel is also much lower than that of the other gels. However, both NIPA and DMA gels exhibit similar retardation times τ ($\sim$ 100 s) and recoverable deformations γ % ($\sim$ 75 %)

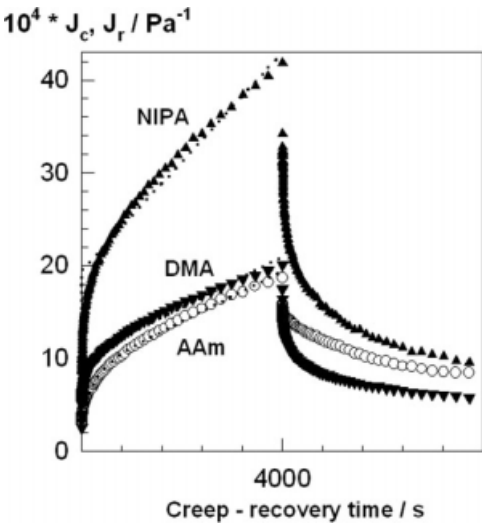

Figure 6 Creep-recovery curves of nanocomposite hydrogels with 6% Laponite for $\gamma_{max} = 0.093 \pm 0.008$. NIPA (▲, $\tau_0 = 20$ Pa), DMA gels (▼, $\tau_0 = 50$ Pa), and AAm gels (○, $\tau_0 = 50$ Pa).

indicating that their microstructures and relaxation processes are similar.

In contrast, however, time-dependent response of AAm gel is distinctly different from the other gels (Fig. 6 and Table I). The retardation time τ of AAm gel is about twice that of DMA or NIPA gels and its irrecoverable compliance is also much higher. We must note that the second term of eq. (1), i.e., the Kelvin–Voigt element represents that part of the structure, in which secondary bonds are breaking and reforming during the experiment.[21] Different values of the retardation time τ thus relate to different types of these bonds in AAm and DMA or NIPA gels. τ corresponds to duration of fluctuations of polymer chains between crosslinks and it normally increases with decreasing crosslink density. Although both DMA and AAm gels have similar viscosities and crosslink densities, the results demonstrate the mobility of the crosslink zones in AAm gels so that longer times are needed for polyacrylamide chains to recover their equilibrium conformations. As a consequence, a large amount of energy is dissipated during the deformation of nanocomposite hydrogel based on AAm; its recoverable deformation is only 56%, as compared to about 75% found for the other gels (Table I).

Different gelation kinetics and viscoelastic responses of AAm and DMA (or NIPA) gels imply different extent of interactions between the clay particles and the monomers. To highlight these interactions, viscosity measurements were conducted on Laponite dispersions containing the monomers. The concentrations were taken as those used in the gelation experiments. The results are given in Figure 7, where the viscosity η of 6% Laponite dispersions containing 5 w/v % monomer is plotted against the shear rate $\dot{\gamma}$. Although the addition of AAm does not change the viscosity, addition of DMA or NIPA significantly decreases the viscosity of the clay dispersion. A decrease in the viscosity of aqueous Laponite dispersion caused by adding NIPA monomer was observed before by Haraguchi et al.,[6] and indicates decreasing extent of clay–water interactions. Thus, DMA and NIPA cover the surface of the clay particles so that their interactions with water molecules are reduced. However, according to Figure 7, AAm–clay particle interactions are too weak to be detected by the viscosity measurements.

Our experimental results thus demonstrate that DMA and NIPA monomers as well as their homopolymers are adsorbed on Laponite particles much stronger than AAm, or its polymer. The influence of the hydrophobic groups on the adsorption of hydrophilic polymers on Laponite surfaces was recently observed in aqueous solutions of poly(ethylene oxide)–poly(propylene oxide)–poly(ethylene oxide) (PEO–PPO–PEO) triblock copolymers; the copolymer adsorbs on the particles via preferential segregation of hydrophobic PPO segments, with hydrophilic PEO segments dangling into the solution.[22] Further, Aubry et al.[23] reported that the amount of hydrophobically modified hydroxypropyl guar adsorbed on the Laponite particle at the surface saturation is about 30% higher compared to the unmodified polymer. Thus, our experimental observations can be explained according to the following scenario (Fig. 8): At concentrations around the critical overlap concentration c* of Laponite, the nanoparticles form several agglomerates in aqueous dispersions. As both DMA and NIPA monomers are adsorbed onto the

TABLE I
Results from the Analysis of the Creep Compliance Curves of Nanocomposite Hydrogels with 6% Laponite by Means of eq. (1)

Laponite gel	$10^4 J_0$/Pa	$10^4 J_1$/Pa	τ/s	10^{-6} η/Pa.s	γ%
NIPA	10.2 (0.1)	9.3 (0.3)	91 (7)	1.7 (0.04)	78
DMA	5.6 (0.1)	4.6 (0.2)	107 (10)	3.7 (0.1)	71
AAm	3.8 (0.04)	4.7 (0.1)	256 (17)	3.7 (0.1)	56

$\gamma_{max} = 0.093 \pm 0.008$, γ% is the recoverable deformation after the creep-recovery test. The values in parenthesis are the standard deviations.

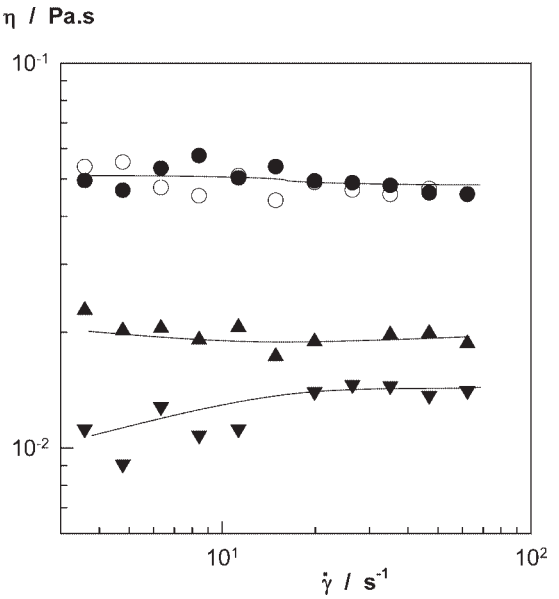

Figure 7 Viscosities η of 6% Laponite dispersions in the absence (open symbols) and in the presence of 5 w/v % AAm (●), DMA (▲), and NIPA (▼).

surfaces of clay particles (Fig. 7), the polymer chains start to grow mainly from the surfaces of the individual particles and their agglomerates. As the lifetime of a growing radical in free-radical polymerization is usually less than 1 s, polymer chains immediately start to form. As the chain ends strongly bind the particle surfaces, instantaneous formation of bridges between the particles lead to the rapid increase in G' and G'' within a short period of time (Fig. 1). As the polymerization reactions proceed, that is, as the number of polymer chains increases, the particle surfaces exhibit an unequal distribution of polymer concentration due to the fact that the region between the nearby particles within the agglomerates are excluded from the polymer. This leads to an unbalanced osmotic pressure pushing the particles further together. This type of interparticular attraction forces is called depletion attractions.[24,25] Thus, the newly formed polymer chains can only cover the surface of the agglomerates so that the polymer is distributed more and more unevenly on the particles resulting in an increase in the cluster density due to the increasing extent of depletion attractions. As a consequence, the crosslinks localized within the clusters lost their efficiencies so that the crosslink density, i.e., the elastic modulus decreases with increasing polymerization time. This situation corresponds to the formation of the nanocomposite hydrogels using DMA or NIPA monomers, as shown in Figure 8. However, in the presence of AAm monomer, the polymer chains start to grow mainly from the solution so that the nanoparticles are not disturbed initially and the moduli gradually increase as the number of chains increases. Although, at longer reaction times, the particles are also subjected to depletion interactions due to the high polymer concentration, these interactions are expected to be weak due to the weak polymer–clay attractive interactions. Weak AAm–clay interactions are also responsible for much stronger viscous behavior of the resulting nanocomposite hydrogels compared to those obtained using DMA or NIPA monomers.

Further proof of this scenario has come from the swelling kinetics of nanocomposite hydrogels. As the gel swells, that is as the nanocomposite material is diluted, one may expect that the chains will move apart to assume a new equilibrium state in the gel solution. This would lead to the separation of the individual clay particles from the agglomerates leading to an increase in the crosslink density of the nanocomposite hydrogel. Indeed, such a behavior was recently observed in nanocomposite hydrogels immersed in water.[12]

The results thus explain the mechanical instability of the nanocomposite hydrogels prepared from AAm monomer compared to those based on DMA

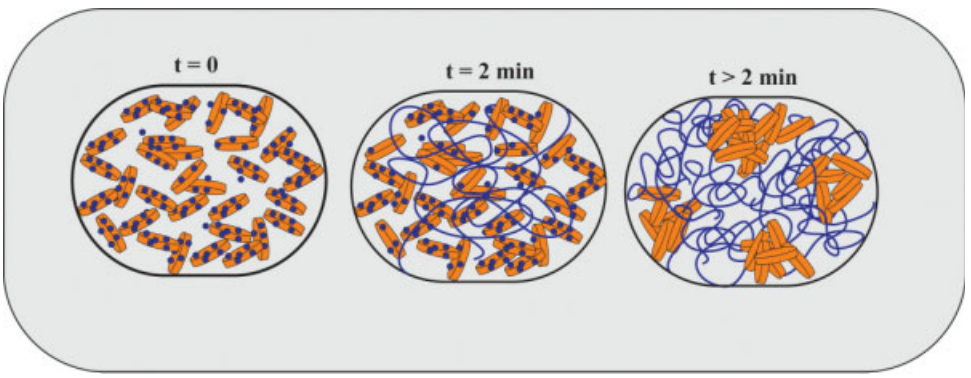

Figure 8 Cartoon demonstrating the polymerization of DMA or NIPA in the dispersion of clay particles to form nanocomposite hydrogels. Only a part of the nanocomposite hydrogel is drawn for clarity. Disks: Laponite particles. Circles: DMA or NIPA monomers. Curves: Polymer chains. [Color figure can be viewed in the online issue, which is available at www.interscience.wiley.com.]

or NIPA monomers. We have to mention that the initial monomer concentration was set to 5 w/v% throughout this study. Recently, formation of nanocomposite AAm hydrogels with good elastic properties and a high degree of toughness was reported at a higher AAm concentration ($\geq$10 w/v%).[11] This is probably due to the increasing number of contacts between the particles and the polymer segments with increasing monomer concentration so that the polymer chains may also grow from the surface of the particles.

CONCLUSIONS

Nanocomposite hydrogels were prepared via *in situ* polymerization DMA, NIPA, and AAm monomers in aqueous dispersions of Laponite. Gelation reactions were monitored by rheometry using oscillatory deformation tests. The gelation profile of AAm polymerization obeys typical gelation kinetics, i.e., both moduli and *tan* δ gradually increase with increasing reaction time and then, they approach plateau values at longer times. However, a reverse behavior was observed during the DMA or NIPA polymerizations; after an abrupt increase in elastic and viscous moduli at the start of the reaction, they both decrease continuously during the gelation reactions. Comparison of the mechanical spectra of the nanocomposite hydrogels shows that, in the high frequency range, the viscous modulus G'' of AAm hydrogels increases with increasing frequency, which reflects fast relaxation processes and is typical viscous behavior of gels formed by temporary junction zones. Creep-recovery tests indicate that the time-dependent response of nanocomposite AAm gel is distinctly different from the other gels. The retardation time of AAm gel is about twice that of DMA or NIPA gels indicating much higher mobility of the crosslink zones in the former gel. As a consequence, a larger amount of energy is dissipated during the deformation of nanocomposite hydrogels based on AAm compared to the other gels. The results were explained with the fact that the hydrophobically modified hydrophilic monomers DMA and NIPA cover the surface of the clay particles before the onset of the gelation reactions while AAm monomer mainly remains in the clay dispersion. As a consequence, weak polymer–clay interaction in AAm gels lead to the formation of gels dissipating larger amount of energy as compared to DMA and NIPA gels.

References

1. Storm, C.; Pastore, J. J.; MacKintosh, F. C.; Lubensky, T. C.; Janmey, P. A. Nature 2005, 435, 191.
2. Calvert, P. Adv Mater 2008, 20, 1.
3. Haraguchi, K.; Takehisa, T. Adv Mater 2002, 14, 1120.
4. Haraguchi, K.; Takehisa, T.; Fan, S. Macromolecules 2002, 35, 10162.
5. Haraguchi, K.; Farnworth, R.; Ohbayashi, A.; Takehisa, T. Macromolecules 2003, 36, 5732.
6. Haraguchi, K.; Li, H. J.; Matsuda, K.; Takehisa, T.; Elliott, E. Macromolecules 2005, 38, 3482.
7. Mongondry, P.; Tassin, J.-F.; Nicolai, T. J Colloid Interface Sci 2005, 283, 397.
8. Mongondry, P.; Nicolai, T.; Tassin, J.-F. J Colloid Interface Sci 2004, 275, 191.
9. Okay, O.; Oppermann, W. Macromolecules 2007, 40, 3378.
10. Abdurrahmanoglu, S.; Can, V.; Okay, O. J Appl Polym Sci 2008, 109, 3714.
11. Xiong, L.; Hu, X.; Liu, X.; Tong, Z. Polymer 2008, 49, 5064.
12. Can, V.; Abdurrahmanoglu, S.; Okay, O. Polymer 2007, 48, 5016.
13. Abdurrahmanoglu, S.; Okay, O. Macromolecules 2008, 41, 7759.
14. Nie, J.; Du, B.; Oppermann, W. Macromolecules 2005, 38, 5729.
15. Annable, T.; Buscall, R.; Ettelaie, R.; Whittlestone, D. J Rheol 1993, 37, 695.
16. Pham, Q. T.; Russel, W. B.; Thibeault, J. C.; Lau, W. Macromolecules 1999, 32, 5139.
17. Tripathi, A.; Tam, K. C.; McKinley, G. H. Macromolecules 2006, 39, 1981.
18. Miquelard-Garnier, G.; Demoures, S.; Creton, C.; Hourdet, D. Macromolecules 2006, 39, 8128.
19. Candau, F.; Selb, J. Adv Colloid Interface Sci 1999, 79, 149.
20. Macosko, C. W. Rheology, Principles, Measurements and Applications; Wiley-VCH: New York, 1994.
21. Barry, B. W. J Colloid Interface Sci 1968, 28, 82.
22. Nelson, A.; Cosgrove, T. Langmuir 2005, 21, 9176.
23. Aubry, T.; Bossard, F.; Moan, M. Langmuir 2002, 18, 155.
24. Poon, W. C. K. J Phys Condens Matter 2002, 14, R859.
25. Piech, M.; Weronski, P.; Xu, X.; Walz, J. Y. J Colloid Interface Sci 2002, 247, 327.